International Symposium of Research Students on Materials Science and Engineering
December 20-22, 2004, Chennai, India
Department of Metallurgical and Materials Engineering, Indian Institute of Technology Madras

CHALLENGES IN PLASMA SPRAY ASSEMBLY OF NANOPARTICLES TO NEAR NET SHAPED BULK NANOSTRUCTURES

V.Viswanathan, Soon-Jik Hong, K. Rea, S. Deshpande, S. Patil, P. Georgieva, T. McKechnie* and S. Seal
Surface Engineering and Nanotechnology Facility & Plasma Nanomanufacturing, AMPAC
and
Department of Mechanical, Materials and Aerospace Engineering,
University of Central Florida, Orlando, FL. 32816-2450, USA
** Plasma Process Inc., Huntsville, Al*

ABSTRACT

Plasma spray processing has been developed to consolidate nanoceramics to form Bulk nano components with retained nano features. From powder agglomeration to variation in spray parameters, each step has been engineered towards nano structured retention and property amelioration compared to their conventional counterparts. From the application perspective, a material more renowned in the aircraft application $MoSi_2$-Si_3N_4-SiC has been selected. Thorough characterization confirmed the retained nano structures using a combined FIB-HRTEM tool. Keeping in mind, the toughness requirements, the ceramic bulk nano structures have been characterized for their Hardness and Fracture toughness. The bulk nanocomposite showed excellent high temperature oxidation resistance. Furthermore, the electronic structure of the composite was studied using the ab-initio QM principles and the DFT theory. The changes in the density of states and the band structure, together with the decreased Fermi energy and the total energy of the reinforced $MoSi_2$ system were calculated and related to its superior mechanical and physical properties.

Keywords: Plasma, Free forms, $MoSi_2$-Si_3N_4, Hardness, Fracture Toughness.

1. INTRODUCTION

Plasma spray technology, a method predominantly used in industries for high temperature coatings has been exploited to produce bulk nanoceramic free form parts which require no machining[1-4] . The plasma particle interaction depends on various factors such as particle size, impingement velocity, amount of heat input to the material, the emissivity of the material to be sprayed[5-6]. Gases used for producing plasma, their proportion, material to be sprayed, particle size and gun design are some of the critical issues that needs to be addressed before the part is made. From the application perspective, a material more renowned in the aircraft application $MoSi_2$-Si_3N_4 has been selected. Characterization for nanostructure retention and mechanical properties such as hardness and fracture toughness has been carried out and compared with Density Functional Theory (DFT) calculations.

2. EXPERIMENTAL

A self explanatory flow chart as shown in Fig.1 depicts all the experimental work that has been done. Nano sized 50 wt% Si_3N_4-$MoSi_2$ powder and 50 wt% micro (20 μm) $MoSi_2$-4%SiC powder was prepared and blended using conventional ball-milling techniques and further

agglomerated in the range of 10-30 μm. The nano-micro mixed $MoSi_2$-Si_3N_4-SiC powder was sprayed using a Praxair Surface Technologies (Indianapolis, IN) SG 100 gun. Fig. 2 shows a plasma spray formed cylindrical near-net-shape bulk reinforced $MoSi_2$ nanocomposite with an inner diameter of 1 inch, outer diameter of 1.25 inch and a height of 1.5 inch. The relative merits and demerits of each of these preparation steps can be gathered from the flow chart.

A detail characterization of the spray-formed bulk nanocomposite was performed using several analytical tools such as XRD, SEM, TEM, and Vickers hardness testing. Vickers hardness measurements were performed on a Shimadzu HMV-2 Vickers hardness tester using a Vickers indenter with a load of 19.6 N applied for 15 s. The fracture toughness of the nanocomposite was calculated using a technique described in literature[12]

A FEI (Hillsboro, OR) 200 TEM-FIB (Focused Ion Beam) equipped with a 25-50 kV gallium liquid metal ion source (LMIS) was used for preparing thin TEM specimens from the spray-deposited nanocomposite. Scanning Transmission Electron Microscopy (STEM) measurements were performed to observe the retention of nanosize grains, their morphology, and physical phenomenon occurring in the spray-formed nanocomposite structures.
Thermal cycling study was performed in the dry air to investigate the high temperature oxidation behavior of the spray formed composite component. The ring type sample was machined from the spray deposited $MoSi_2$-Si_3N_4-SiC shell and subjected to 1100^{o}C for 10, 50, 100, 200 hours. The mass change is recorded using a balance connected to the oxidation furnace to monitor the oxidation kinetics.

3. RESULTS AND DISCUSSION

The science behind bulk nanomanufacturing, experimental outcome in the form of microstructures, the mechanical properties that are measured are discussed at length in this section.

3.1 Issues behind Bulk Manufacturing of Nanostructures

3.1.1 Plasma-Particle Interaction

Plasma-particle interaction results in the formation of atoms in excited state, ground state, ions, and photons in the plasma plume. As a result of these atomic dissociation and recombination processes, particle that is sprayed is taken to a partial molten state for a brief period of time till it splats on to the substrate. Within this period of time if the particle size is below a threshold size, it may get evaporated. Moreover, knowledge of emissivity of the material to be sprayed is also important. Ceramics usually have a high emissivity so that the amount of radiative heat emitted is high compared to the metallic particles. The range of emissivity for $MoSi_2$ is 0.7-0.9. $MoSi_2$ finds important industrial application as a heating element and also loses heat easily through radiative heat transfer. For nanostructure retention, emissivity property can be a point of merit as too much of heat is going to cause abnormal agglomeration which hampers the very purpose of nanostructure retention. So, emissivity can be a key factor in retaining the nanostructures.

The amount of time that particle stays in the flame can be controlled using a flexible gun design. The powder port being used to inject the particle can be angled in different ways as to suit the needs[7]. With the help of this channel, the powder can flow along the plume, against the plume or any specific direction. Particle agglomeration can be avoided to maximum possible extent if the particle is sprayed along the plume so that the interaction between them can be kept minimal. Again, it is necessary to strike a balance, as too low an interaction may affect the density of the product.

The primary way of heat transfer between the particle and the plasma is through conduction. Conduction, per se depends on the ingenious selection of gases for producing the plasma flame[8]. Diatomic gases such as Nitrogen and Hydrogen have high heat conducting potential compared to monoatomic gases. Higher enthalpies associated with the reaction, helps to conduct the heat to the particle and melt it subsequently. Ar and He, being monoatomic gases are deemed suitable for this process especially for nanostructure retention. The reason being the fact that higher heat conducted to the particle can effect coarsening.

3.1.2. Coating Vs Free forms – Engineering Aspects

Substrate is engineered to facilitate easy removal of the part. This is in contrast to the substrate preparation required for hard ceramic coatings. A tensile stress on the sprayed part and a compressive stress on the substrate is essential for obtaining a free form part. Aluminum substrate can facilitate the removal by shrinking more, compared to steel. High Velocity Oxy fuel (HVOF), another technique used for making hard coatings might not be suitable for part removal, as it is more or less like a shot peening technique which will nullify the shrinkage stresses generated in the substrate due to particle solidification and give rise to good bonding[9] Cooling and solidification of most materials is accompanied by contraction or shrinkage. As particles strike they rapidly cool and solidify. This generates a tensile stress within the particle and a compressive stress within the surface of the substrate. As the coating is built up, so are the tensile stresses in the coating. With a lot of coatings a thickness will be reached where the tensile stresses will exceed that of the bond strength or cohesive strength and coating failure will occur. Increase in the tensile stresses is sufficient to remove the part easily from the substrate.

3.2 Microstructure Evaluation Using Optical Microscopy, FIB and HRTEM

The trial for spraying nano ceramic particles through plasma flame has been successful and a composite made of $MoSi_2$-Si_3N_4-SiC cylindrical bulk nanocomposite without any defects on the surface was manufactured using plasma spray technique. The relative density of the nanocomposite was about ~85 %. The Si_3N_4 particles was uniformly distributed within the $MoSi_2$ matrix with average sizes of 15 □m in the inner, 10 □m in the outer and less than 5 □m in the middle region of the cylinder.

3.2.1 Optical Microscopy

The distribution of the Si_3N_4 particles in the matrix was observed by the optical micrograph (Fig. 3). It can be seen that the fine Si_3N_4 particles (black color) are homogeneously distributed in the $MoSi_2$ matrix. Microstructures have been analyzed from the ID to the OD and the size and shape change of the Si_3N_4 particles is noticed. It can be seen that the shape of the Si_3N_4 particles is elongated and the size is larger at the inner diameter of the cylinder compared to middle and outer diameter of the cylinder. In the middle portion, homogenous distributions of particles were observed. The microstructural variations are attributed to the amount of heat transferred to the particle by the gases, the amount of heat radiated by the particle to the gas, substrate temperature. As discussed above, the amount of heat transferred to the particle can be increased by channeling the powder port. Radiation heat emitted out of the particle is a factor which is material specific and nothing much can be done once the material system is selected for spraying.

3.2.2 Focused Ion Beam (FIB) and HRTEM

Fig. 4(a) and 4(b) shows an STEM image and TEM image respectively of the microstructure of the spray-formed component. The micrographs clearly show $MoSi_2$ grains (white) and the fine homogeneously dispersed Si_3N_4 nanoparticles. In some areas the Si_3N_4 nanoparticles were agglomerated. The size of the $MoSi_2$ in coarse area varied between 0.5 and 1 μm and the Si_3N_4 particles were in the range of 30-100 nm.

In addition to the plasma particle interaction that is predominantly responsible for the particle growth, amount of carrier gas being fed to the spray gun also has an effect in dwell time. More carrier gas feed rate will push the particle through the gun thereby keeping the dwell time low. More the dwell time, the more is the particle coarsening. A process such as Hot Isostatic pressing does not have these many process parameters to effectively control the grain size. Clearly, plasma has more operating freedom than any other conventional ceramic processing techniques. Similar microstructure was also observed in hot isostatically pressed $MoSi_2$-Si_3N_4 ceramics pellets[10], however the particle sizes (e.g. 200-1000 nm of $MoSi_2$ and 500-1000 nm of Si_3N_4) were larger than the present research. Hence, it is clear that such uniformly distributed nanoparticles in the $MoSi_2$ matrix enhance the mechanical properties of the plasma spray formed composite.

3.3 Mechanical Property Evaluation using Vickers Hardness Tester

Hardness and Fracture toughness of the part has been measured and plotted below.(Fig.5)

3.3.1 Hardness

As discussed above, the microstructure of the plasma-formed component varies as a function of the component's wall thickness. Thus, as a result, the mechanical properties such as Vickers hardness and fracture toughness were found to vary also, as shown in
Fig. 5. We believe that the different values of the Vickers hardness might be associated with the different distribution and the size of the Si_3N_4 particles in the $MoSi_2$ matrix. Despite the large percent porosity of the plasma sprayed component, as expected, its mechanical properties increase due to the nanosized Si_3N_4 particles and their relative homogeneous distribution in the matrix.

3.3.2 Fracture Toughness

The fracture toughness of the nanocomposite was measured by the Vickers hardness indenter. The average room temperature fracture toughness of the nanocomposite was ~7 MPa $m^{1/2}$. Furthermore, the fine microstructure in the middle region of the cylinder showed relatively higher fracture toughness than the other regions of the composite. Thus, it brings once again the importance of reinforcing of the $MoSi_2$ based materials toward increasing their strength, as already reported elsewhere[11].

3.4. Oxidation Kinetics of the Nanocomposite

Fig. 6 shows the outcome of the oxidation study of the $MoSi_2$ reinforced composite. In the first five hours, oxidation of SiC resulted in the reduction in net weight gain of the sample. The oxidation kinetics then saturates after 100 hrs exposures. During the first cycle, rapid oxidation of the surface is due to the formation of SiO_2 resulting in weight gain. Partial increase in mass gain at early stages may be attributed to the increase in the exposed surface porosity.

At higher temperatures, a thin continuous protective oxide (SiO_2) layer forms, corresponding to very small weight gain over a long period of time. However, the oxidation rate at 200 h was found to decrease. One possible reason could be related to the evaporation of MoO_3. Thus, the volatility of MoO_3 plays an important role in the oxidation behavior of $MoSi_2$. At elevated temperatures (>1000 ^oC), MoO_3 vaporizes and the diffusion of Si is rapid enough to form a continuous protective oxide scale, which effectively seals the surface[13]. In the temperature range of 600-1100 ^oC, $MoSi_2$ exhibits a thin oxide layer on the surface due to internal oxidation of Si. A competition between SiO_2 formation and MoO_3 volatilization occurs, keeping the mass gain in the range of ± 1 mg/cm^2. Furthermore, such a high oxidation resistance at 1100 ^oC is due to the presence of a high volume percent Si_3N_4 which affects the suppression of the rapid oxidation of Mo and SiC particles. Pesting, indiscriminate oxidation prevalent in monolithic $MoSi_2$ is absent in the plasma sprayed $MoSi_2$-Si_3N_4 composite which goes to show that plasma processing can just be another processing method for high oxidation resistant ceramics.

4. MATERIALS SELECTION AND PROPERTY EVALUATION - A SIMULATION STUDY

In order to fully understand the enhanced mechanical properties of the $MoSi_2$ reinforced composite, it is necessary to combine this experimental study with the theoretical ab-initio calculations. Therefore, the present simulation study is with the purpose to study the changes in the electronic configurations, the final energy and the consequent mechanical and physical properties of $MoSi_2$ when reinforced with Si_3N_4 and SiC.

4.1 Total Energy Optimization

Fig. 7 shows an energy dispersion curve calculated using a Materials Studio package based on the Quantum Mechanics and Density Functional Theory Principles. It can be seen that the addition of SiC to the $MoSi_2$, decreases the total final energy of the resultant system from –2142 eV to the –5333.19 eV. This indicates the stability of the structure of the $MoSi_2$-SiC composite and subsequent improvement in the mechanical properties.

According to the DFT model, the total energy of a system of electrons can be articulated as a function of their electron densities. If □ is the charge density, the total electron energy, E_t[□], can be expressed as the sum of the kinetic energy of the noninteracting particles, T [□], the Coulomb energy due to the electrostatic interactions among all the charged particles in the system, U [□], and the exchange-correlation energy, E_{xc}[□] respectively.

In an N-atom system, we introduce □V_e, □V_N and V_{NN} as the electron-electron repulsion, electron-nucleus attraction and nucleus-nucleus repulsion, respectively for U component and calculate the total energy contribution from its components

$$E_t[\rho] = \sum_i \left\langle \phi_i + \left| \frac{-\nabla^2}{2} \right| \phi_i \right\rangle + \left\langle \rho(r_1) \left[\varepsilon_{XC}[\rho(r_1)] + \frac{V_e(r_1)}{2} - V_N \right] \right\rangle + V_{NN}$$

where □$_i$ is the sum of all occupied molecular orbitals.

4.2 Effect of Reinforcement

Alongside, the addition of Si_3N_4 to the $MoSi_2$ further decreases the total energy to –5208.21 eV. From Fig. 7, it can be deduced that with the presence of both Si_3N_4 and SiC in $MoSi_2$ matrix, the final energy of the composite is even decreased to –6256.18 eV. It clearly shows the consequences of the coexistence of all the phases and the electron distribution in the resulting structure. It can be understood that as a result of the interaction between the heterogeneous

particles, the final energy is reduced and the attractive forces are increased. Thus, the heterophase interfaces with low energy correspond to the stable reinforcing bonding, high temperatures creep resistance and high temperature strength.

As discussed in the above experimental and theoretical investigations, the mechanical properties of the $MoSi_2$ matrix improve with the addition of Si_3N_4 and SiC reinforcement. However, we believe that with an increase in the density of $MoSi_2$-Si_3N_4-SiC nanocomposite by optimum processing conditions, a further increase in fracture toughness and related properties are expected.

5. CONCLUSIONS

Based on our experience, plasma processing is proved to be a handy tool whose parameters can be manipulated at will to achieve the end product with desired properties. The process can be further optimized to be cost effective for bulk production of composites. The successful consolidation of near-net-shape $MoSi_2$-Si_3N_4-SiC bulk composites with retained nanostructure using plasma spray forming is reported. The average fracture toughness of the bulk nanocomposite was as high as ~7 MPa $m^{1/2}$which was associated with the homogeneous distribution and the retention of nanostructures. In addition to the experimental studies, the final energy of the composite was calculated using ab-initio methods. The final energy values were minimized due to the addition of SiC and Si_3N_4 reinforcements and subsequent increase in the mechanical properties of the $MoSi_2$ matrix. The oxidation study of the nanocomposite shows that during the initial stages of exposure at 1100 ^oC the oxidation is accelerated due to SiO_2 formation, however, insignificant mass change is observed during long term exposures. Finally, our further research is directed toward optimizing the plasma forming parameters for fabrication of the bulk free form parts with higher density and enhanced mechanical properties.

ACKNOWLEDGEMENTS

The authors are thankful to the Office of Naval Research Young Investigator Award Program. ONR N00014-02-1-0591, the funding agency and Plasma Process Inc. Huntsville, Alabama for the assistance in plasma spraying. Authors also thank Dr. Suryanarayana for supplying the $MoSi_2$ and Si_3N_4 nanopowders. We also thank UCF DURIP plasma nanomanufacturing N00014-02-1-0858.

REFERENCES

1. C.C. Berndt, J. Therm. Spray Technol., 10 (1) (2001), 147-182.

2. He J.; Ice M.; Schoenung J.M.; Shin D.H.; Lavernia E.J., J. Therm. Spray Technol., 10(2) (2001), 293-300.

3. A. Agarwal and T. Mckechnie, NASA Goddard Space Flight Center, Technical Report NAS5-0008, November (2001).

4. A. Agarwal, T. Mckechnie, and S. Seal, J. Therm. Spray Technol., 12(3) (2003), 350-359.

5. K. Ramachandran, V. Selvarajan, Computational Materials Science 6 (1996) 8l-91.

6. R. Ramasamy, V. Selvarajan, Computational Materials Science 15 (1999) 265-274.

7. R.F. Bunshah, Handbook of Hard Coatings, Noyes Publications (2001) ISBN 0-8155-1438-7.

8. Maher I Boulos, Pierre Fauchais and Emil Pfender, Thermal Plasmas, Vol. 1 (1994) Plenum press ISBN 0-306-44607-3.

9. www.gordonengland.co.uk
10. Mohan G. Hebsur, Materials science and Engineering A 261 (1999) 24-37.

11. J. S. Jayashankar, E. N. Ross, P. D. Eason and M. J. Kaufman, Mater. Sci. Eng. A 239-240 (1997), 485-492.

12. G. R. Anstis et al., J. Am. Ceram. Soc. 64 (1981), 533.

13. D. A. Berztiss, R. R. Cerchiara, E. A. Gulbransen, F. S. Pettit and G. H. Meier, Mater. Sci. Eng. A 155 (1992), 165-181.

FIGURES

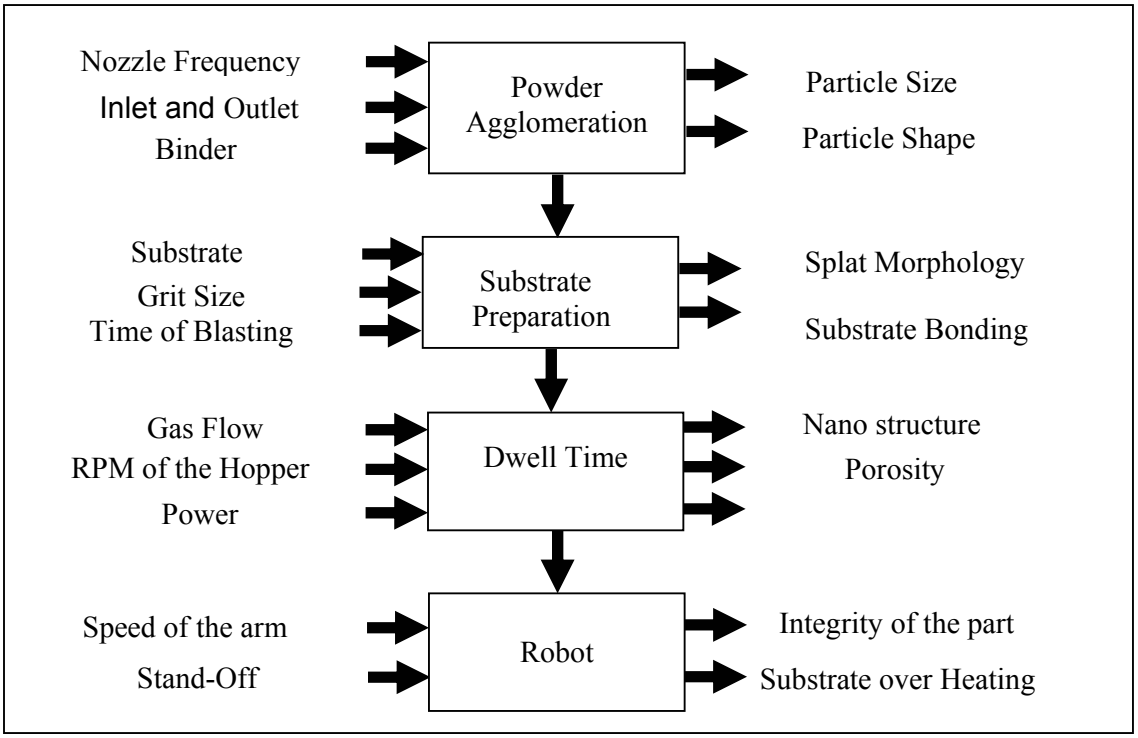

Fig. 1 Flow Diagram revealing the process intricacies that are involved in achieving retained nanostructures

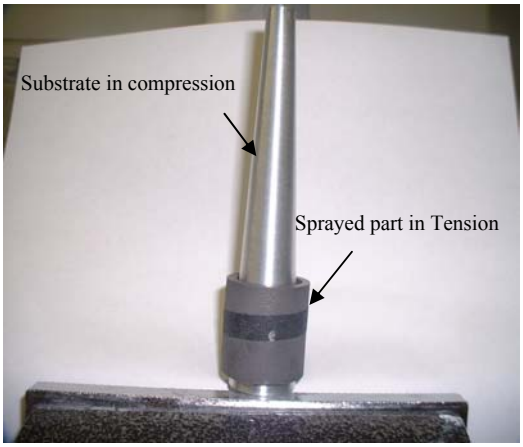

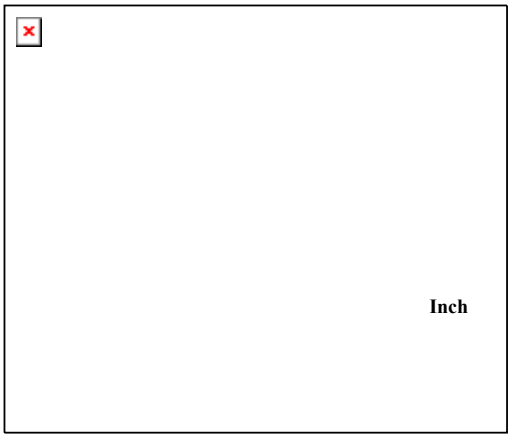

Fig 2(a) The mandrel is subjected to compressive stresses while the sprayed part takes up tensile stress as the build up continues. Fig 2(b) A 1.25" OD X 1 inch ID X 1.5" Length was produced with full integrity.

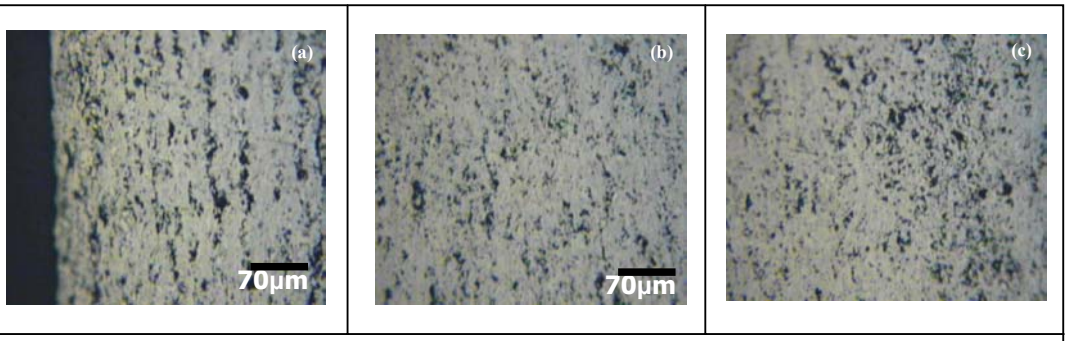

Figure 3. Optical micrographs of the cross section of plasma sprayed bulk nanocomposite with thickness: inside (a), middle (b), and outside of cylinder (c).

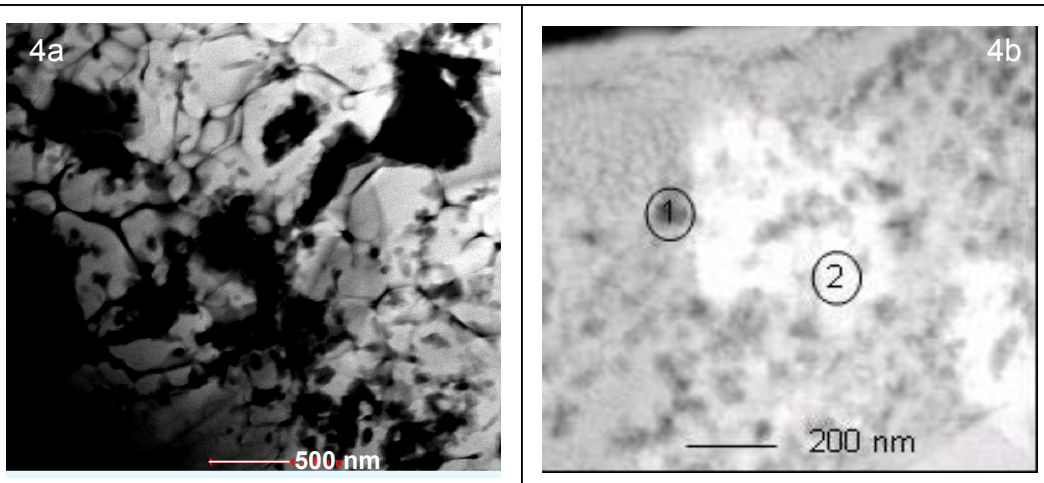

Fig 4a Particles of Si_3N_4 (Dark) showing no appreciable grain growth in the STEM Microstructure compared with Fig 4b TEM microstructure showing (1) (dark) nano $MoSi_2$ phase and (2) (bright) Si_3N_4 phase

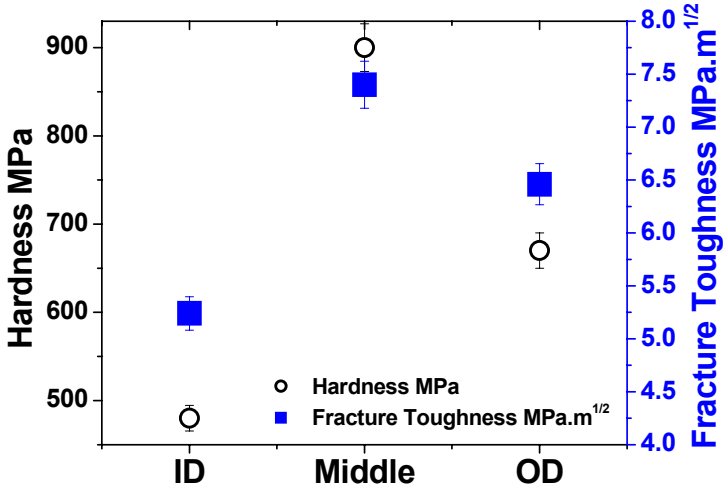

Fig. 5 Mechanical properties of the plasma sprayed part with thickness.

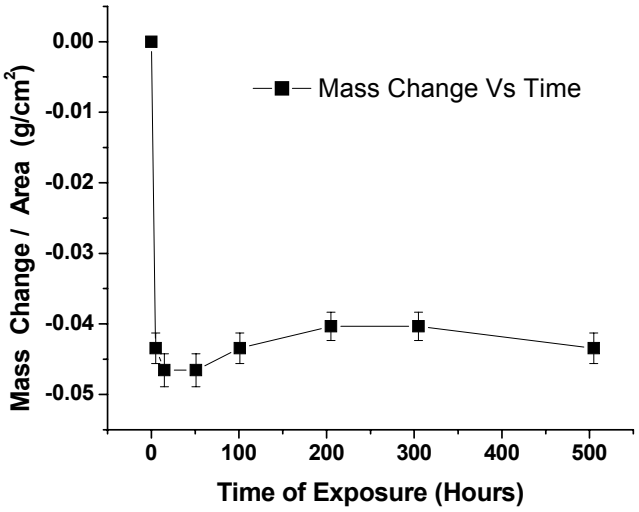

Fig.6 Oxidation kinetics of the nanocomposite exposed at 1100°C in dry air as a function of time.

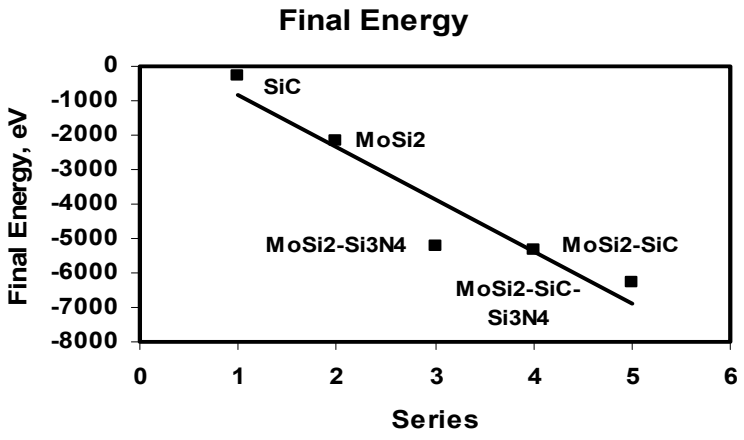

Fig 7. Simulation studies performed on Mosi2 along with other reinforcements showed a decrease in the internal energy of the system which is measure of the stability of the system